

MATHEMATICS OF A CLOCK ESCAPEMENT

Dr. Eng. Gianni Petrangeli

University of Pisa

Via C. Maes, 53, Roma, Italy

g.petrangeli@gmail.com

ABSTRACT

This article intends to offer a full, although as far as possible simple, mathematical treatment (model) of the dynamical behaviour of an escapement. The Graham escapement has been chosen as a reference, but the same model can be adapted to other escapement mechanisms for clocks and watches.

The possible uses of this study are:

- offer an aid to the comprehension of the functioning of this mechanism by interested people,
- lend support to clock and watch design and repair

It has been assumed that the spectrum of readers and of their background could be large, so the initial description of an escapement maybe useless for horologists, while some of the mathematical treatment can be unfamiliar for other readers (as explained in the following, mathematical details which can be overlooked by not interested readers, will be identified in the text).

The mathematical model is described and put to work on an arbitrary and, as will be seen, initially unacceptably imprecise clock. Some deductions and suggestions for modification will be discussed, in order to practically explain one of the possible uses of the model.

Some future developments of this work are described.

1. PREMISE

[The universe] cannot be read until we have learnt the language and become familiar with the characters in which it is written. It is written in mathematical language and the letters are triangles, circles and other geometrical figures.....

(Galileo)

My field of work has been for many years plant engineering, specifically nuclear plant engineering, but since a long time I have been looking, as a matter of pure technical interest, for a mathematical treatment of the wonderful clock escapement mechanism. Since I have not found material simple enough and at the same time complete which could satisfy this technical interest of mine, I have decided to try to work at such a study by myself. This article is the initial product of my effort.

The material which follows intends to offer a full, although simple as far as possible, mathematical treatment (model) of the dynamical behaviour of an escapement.

Its possible uses are:

- aid to the comprehension of the functioning of this mechanism by interested people,
- support to clock and watch design and repair

In the following pages, a mathematical model is presented and put to work on an arbitrary and, as will be seen, initially unacceptably imprecise clock. Some deductions and suggestions for modification will be discussed, in order to practically explain one of the possible uses of the model.

The main mathematical tools used are homogeneous and non-homogenous differential equations, which are usually dealt with in graduation courses. However, the exposure which follows has been made in such a way that makes possible the use of the proposed model to the reader without experience in this field of mathematics. In practice, the reader can jump the differential equations and directly go to their solution in which the numerical constants are to be determined on the basis of the initial conditions of the motion (position and speed). The portions of the mathematical treatment which can be ignored will be identified in the text by a side bar (like the one alongside this paragraph). An high school knowledge of elementary algebra and trigonometry is however needed, as well as the use of a calculation spreadsheet like Excel or Numbers.

2. SHORT DESCRIPTION OF A PENDULUM CLOCK

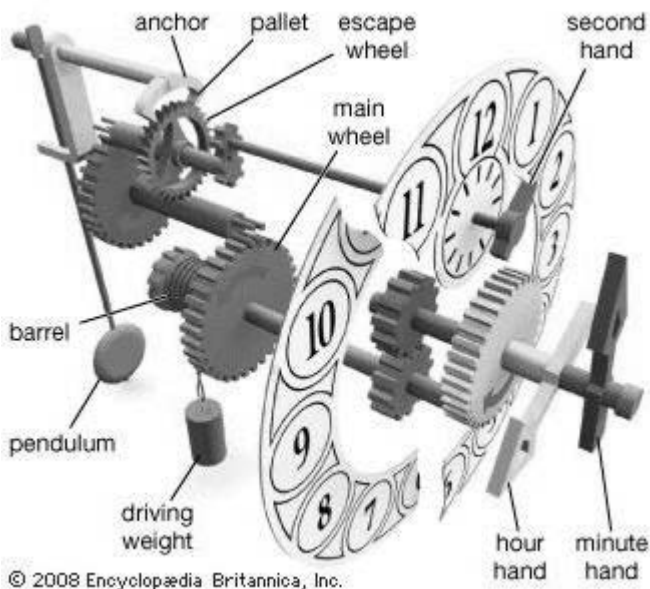


Figure 1. Simplified scheme of a pendulum clock [www.britannica.com,2012]

Apart from the indicator components (dial, hands, etc.), the hart of a pendulum clock is composed of a regulator mechanism (the pendulum with its anchor or crutch) and of an advancement mechanism (escapement wheel and gear train up to the source of power, in Fig. 1 a driving weight

and in Fig. 9 a spiral spring in a barrel). The complex of the two mechanisms will be simply referenced here as “escapement mechanism”. The escapement of the clock shown in Figure 1 has been chosen for generic illustration purposes : the escapement studied in this paper is slightly different (it is a deadbeat, Graham, escapement indeed)

The advancement mechanism (in the absence of the regulator mechanism) tends to run away until it reaches a certain rotational speed, when the motive power is balanced by the dissipated power (mechanical friction and hydrodynamic air friction). This final rotational speed may not be constant, as in the case of a spring-propelled advancement.

The regulator mechanism (the pendulum and anchor complex in a pendulum clock), in the absence of the advancement mechanism, tends to regularly oscillate with a slightly diminishing amplitude in each cycle, due to mechanical and hydrodynamic air friction.

The task of the advancement mechanism is, however, to move the indicator hands with a constant, slow, rotational speed; it, therefore, needs a regulator since the run-away speed (above mentioned) would be in practice too high and , as explained, not constant in some case. In this situation, the advancement mechanism needs a regulator mechanism which is capable of controlling the rotational speed and to make it essentially constant on the average.

On the other side, the regulator mechanism needs a slight help from outside in order to eliminate the continuous decrement of its oscillation amplitude due to friction.

The two above mentioned exigencies are wonderfully satisfied by the coupling of the two mechanisms, advancement and regulator, in one single mechanism, the clock escapement [De Carle 2008, De Carle 2002, Rawlings 1980/1993, Le Lionnais, 1959].

As it will be explained later in more detail and as it can be imagined by the inspection of Fig.1 and of Fig.2, the teeth of the escapement wheel interact in various ways with the pendulum anchor during their motion. A classical Graham Escapement [De Carle 2008] is taken as a reference in this work.

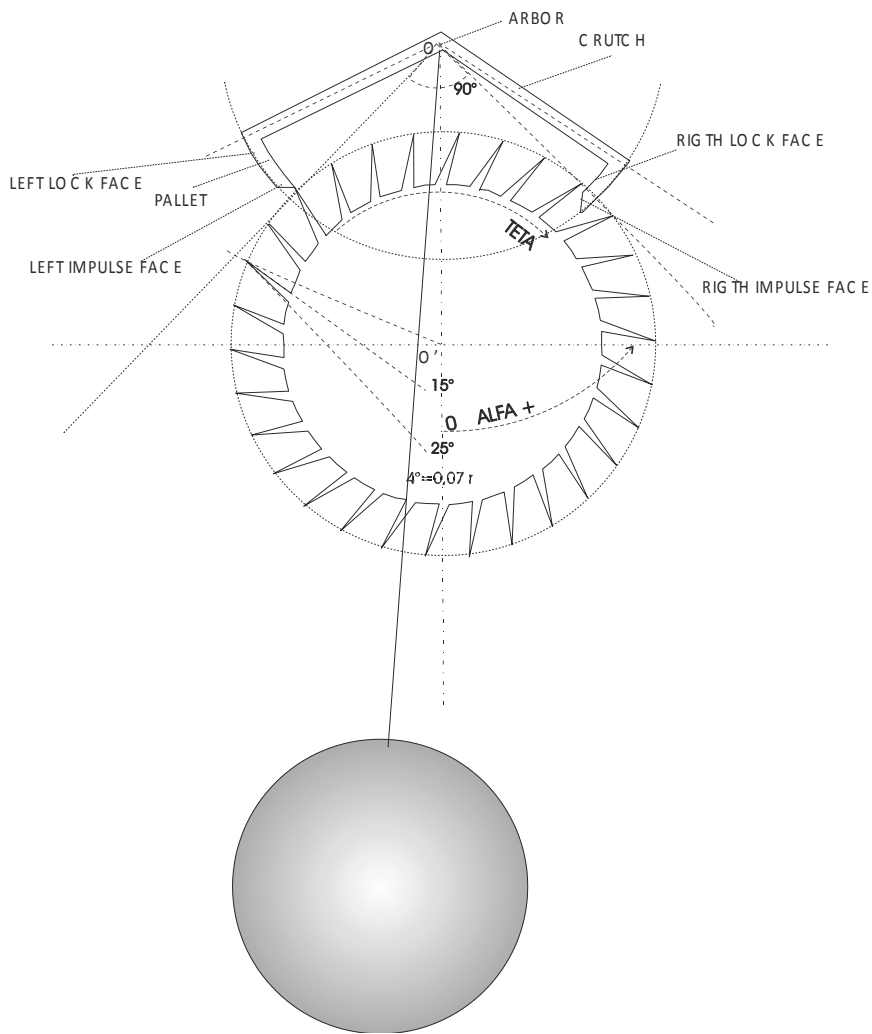


FIGURE 2. Escapement mechanism chosen as a reference in this paper

In particular:

- when an escapement wheel tooth comes in contact with one of the two impulse faces (Fig. 2) of the anchor (or crutch in Fig. 2), the wheel imparts an impulse to the pendulum anchor;
- when the two mechanisms do not interact, the pendulum continues its oscillation freely and the escapement wheel suddenly jumps to the next position of contact with one of the two lock faces of the anchor;
- when a wheel tooth is in contact with one of the two lock faces of the anchor, the wheel itself is stopped for a while and the pendulum is retarded by the contact friction force.

3. PHASES OF THE MOTION OF AN ESCAPEMENT

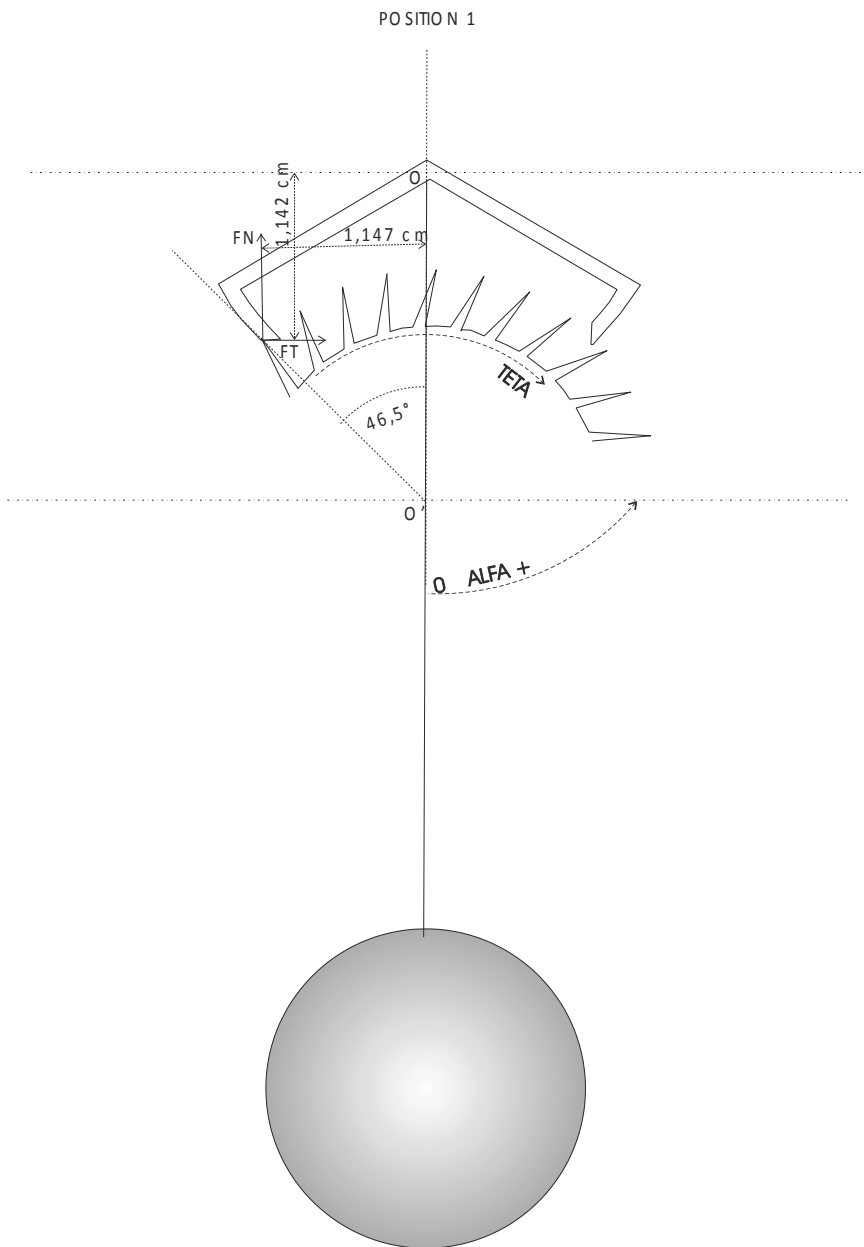


FIGURE 3. Position 1 of the escapement

In this position, the contact between a wheel tooth and the left impulse face of the anchor starts. A pressure force FN and a friction force FT start to be exerted on the impulse face of the anchor.

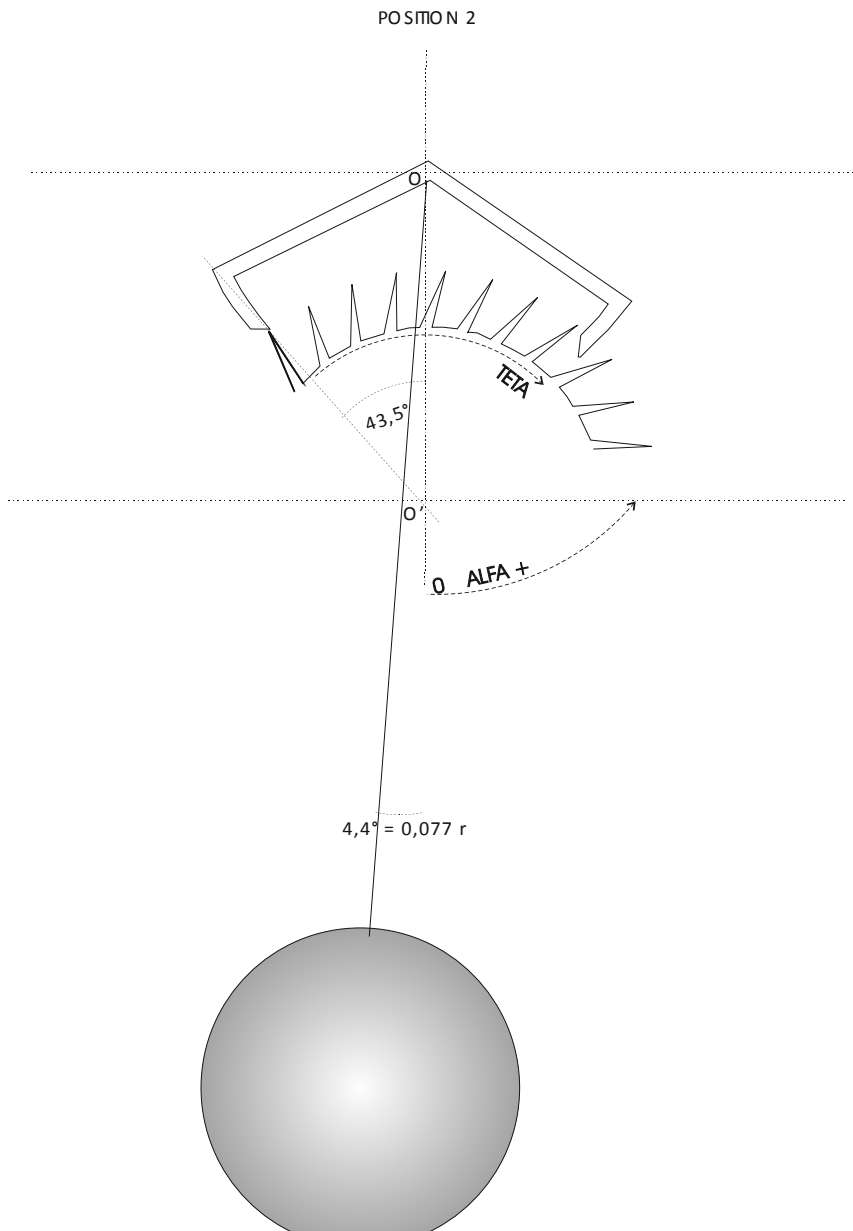


FIGURE 4. Position 2

The left impulse phase ends since the wheel tooth reaches the end of the left anchor impulse face. The pendulum and the escapement wheel start to move independently for a brief period of time, essentially dependent on the runaway speed of the wheel.

POSITION 3

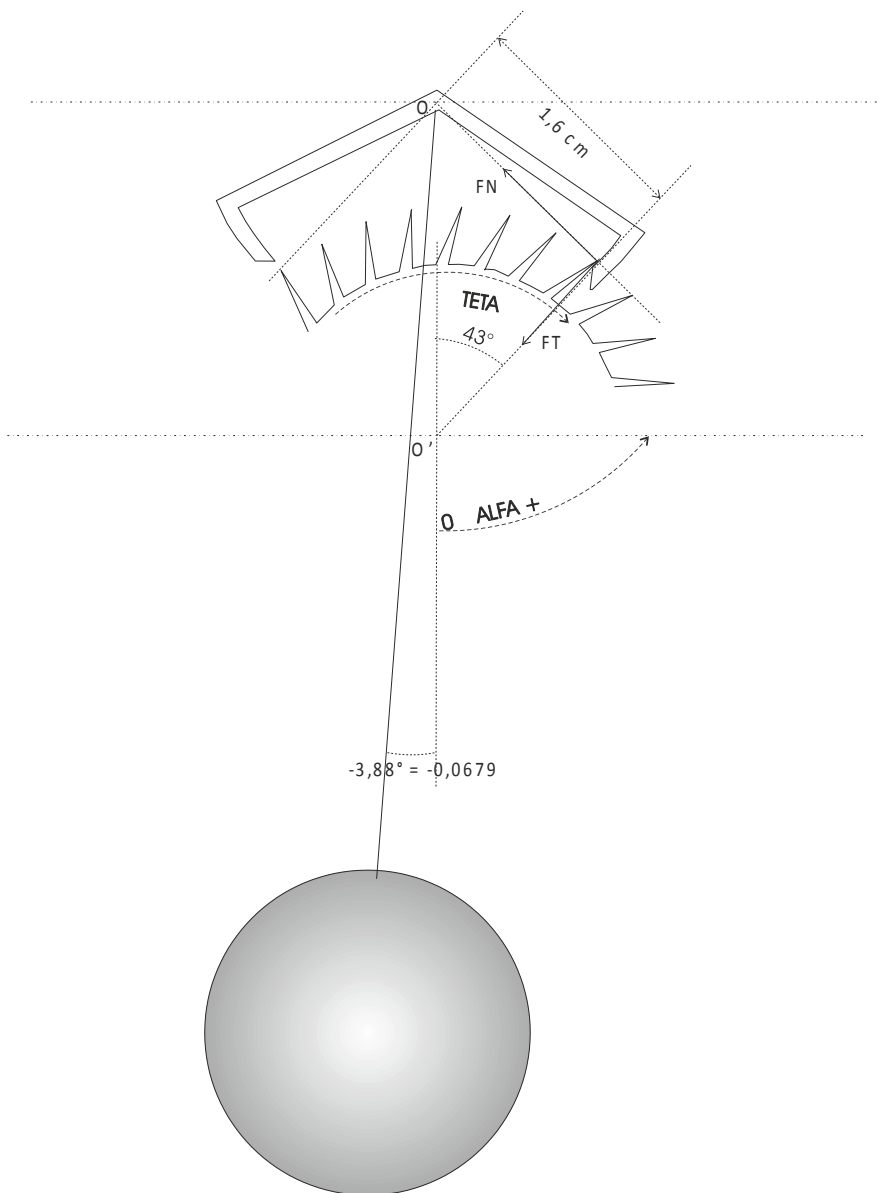


FIGURE 5. Position 3

A wheel tooth impacts the right anchor lock face and its rotation motion ends. A normal to surface force FN and a friction force FT are exchanged between tooth and anchor. FN does not originate any rotation moment over the anchor, since the locking surfaces are arcs of circle (or, more precisely, an arc of cylinder) with centre in the rotation centre O of the anchor. FN gives a non-zero moment around O' with a lever arm of 1,6 cm, indicated in the drawing.

POSITION 4

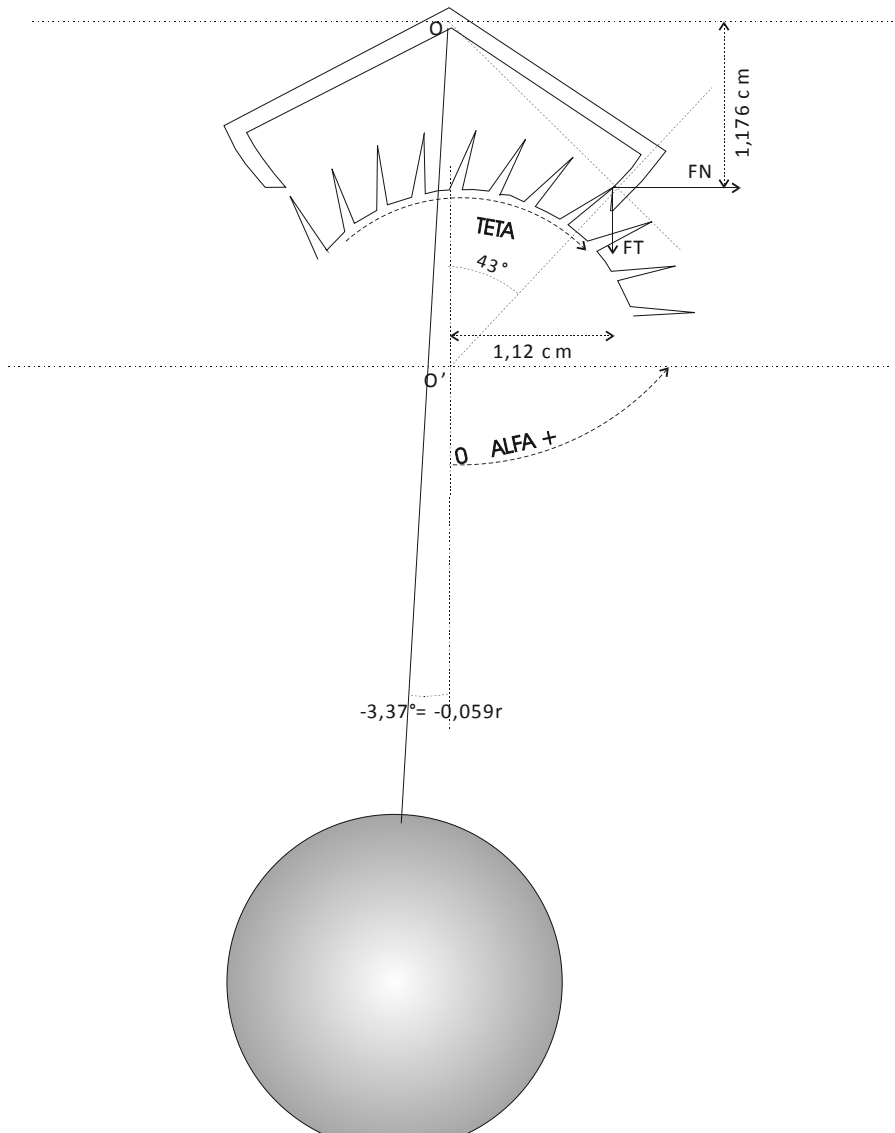


FIGURE 6. Position 4

The lock phase is ended here and the right impulse phase starts. FN and FT both have a non-zero moment around O, with the indicated lever arms.

POSIMON 5

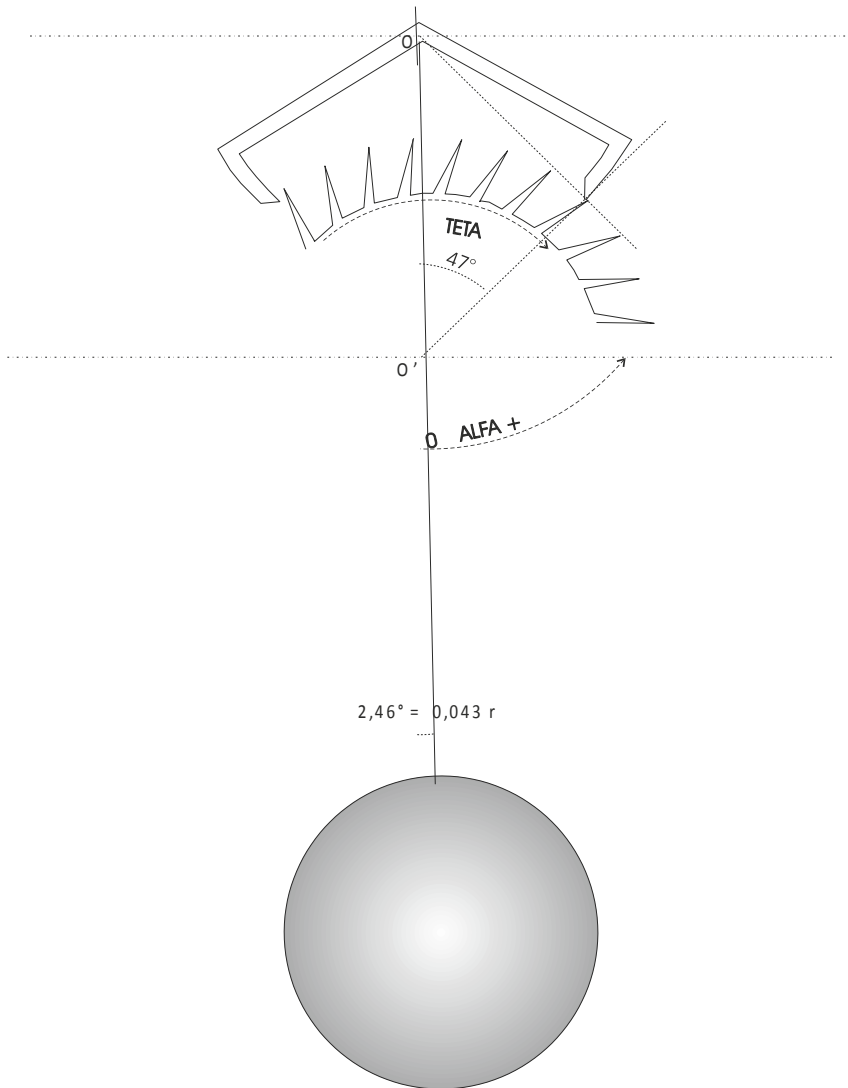


FIGURE 7. Position 5

The right impulse phase ends and the wheel and pendulum are again free to move under the action of their motive power (in our case, a spring, Fig. 9 and the pendulum weight).

POSITION 6

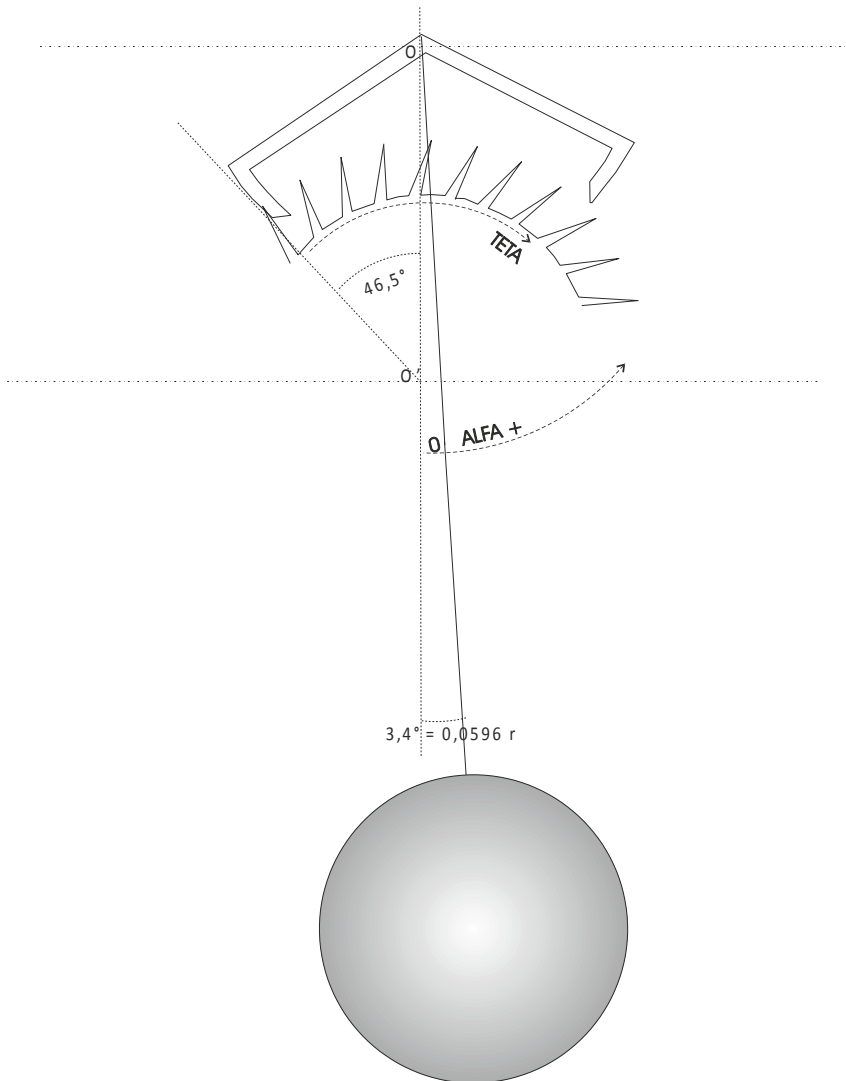


FIGURE 8. Position 6

A wheel tooth impacts on the right lock surface of the anchor and a lock phase (right lock phase) starts which is similar to the left lock phase of Position 3. The lever arm of FT is the same as for Position 3, for symmetry.

The above described six positions of the mechanism define six Phases of its motion:

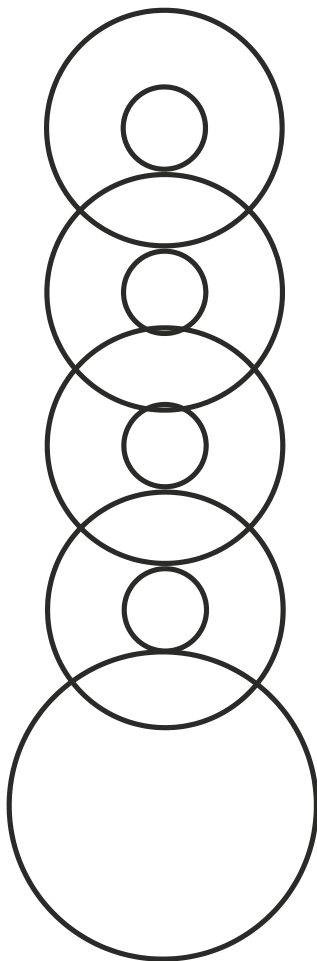
- Phase 1-2, from Position 1 to Position 2: left impulse phase
- Phase 2-3, from Position 2 to Position 3: left free run phase
- Phase 3-4, from Position 3 to Position 4: right lock phase
- Phase 4-5, from Position 4 to Position 5: right impulse phase
- Phase 5-6, From Position 5 to Position 6: right free run phase
- Phase 6-1, From Position 6 to Position 1: left lock phase

The mathematical treatment of the six phases will be given in Section 5.

4. DESCRIPTION OF THE ESCAPEMENT MECHANISM CHOSEN

The escapement mechanism taken here as a reference is a classical Graham Escapement [De Carle, 2008] with a spiral spring as the source of power. This mechanism is frequently used in modern pendulum clocks. The gear train which transmits the motion to the escapement wheel is shown in Figure 9.

The dimensions chosen in this article are deemed to be reasonable for a table pendulum clock and have been taken partly from internet pages and partly from a real clock. A digital centesimal (1/100 mm accuracy) gauge has been used for the measurement of lengths and of angles (through the measurement of appropriate segments). The spring moment at the barrel periphery has been estimated at 21000 g cm. The pendulum has been assumed to be suspended at an elastic leaf spring, considered as free from any energy loss during the motion. The friction factor between the dry surfaces in contact (escapement wheel tooth and pallet locking surfaces) has been assumed equal to 0.08, which is a rather low, yet still possible, value. After some check of significance, the energy loss in the pendulum due to hydrodynamic air friction has been disregarded.



Escapement wheel and pinion:

R= 16.9mm, r= 2.075 mm
30 and 8 teeth, t= 0.8 mm

Seconds Wheel and pinion:

R= 18.44mm, r= 1.85mm
80 and 7 teeth, t= 0.79 mm

Central wheel and pinion:

R= 19.38mm, r= 3.4mm
84 and 10 teeth, t= 1.16mm

Median wheel and pinion:

R= 20.17mm, r= 3.5mm
65 and 10 teeth, t= 1.47mm

Spring Barrel and wheel:

R= 27.37mm
76 teeth

Overall reduction ratio =

= $76/10 * 65/10 * 84/7 * 80/8 =$
= 5928

FIGURE 9. Gear train of the escapement wheel

5. MATHEMATICAL MODEL OF THE MOTION PHASES AND CALCULATIONS

Many books and articles can be found in the open literature on the mathematical treatment of the clock escapement [Beléndez,2007, Gelsey,, Headrick,2012, Lepsckhy, 1992, Moon, 2006, Popkonstantinovich,2011, Schwartz, 2001] yet no simple and complete mathematical model has been presented. Such a model is needed for deeper comprehension of the mechanism functioning and for helping in design and repair. The present work is intended to present one model of this kind, which can obviously be improved and expanded in future. The main object of the work is a clock, although the model can be easily extended to a watch.

The first step in the use of the proposed model is the drawing of the six positions of the mechanism during one motion cycle (Figures 3 to 8). The objective of this work is to determine the pendulum and escapement wheel angles in the six positions on the mechanism.

Figure 2 contains the essential data for this drawing exercise [Headrick, 2012]. First of all, the escapement wheel radius has to be chosen and the teeth of the wheel drawn : in Figure 2, angles of 15 and of 25 degrees have been chosen for each wheel tooth faces, with reference to the pertinent radial segment. The pendulum rotation point has then to be chosen in such a way that the escapement wheel outer circumference is seen from it under an angle of 90°. The line O-O' is vertical. Consequently, the tangency points on the escapement wheel circle from centre O are seen from centre O' under an equal angle of 90° and are symmetrically located with reference to the vertical line. The pallet locking faces (Figure 2) are arcs of circle around the centre O'. The pallet tentative lengths of impulse faces (assumed here, but not necessarily in general, rectilinear segments) can be assumed in such a way that they are seen from the centre O' under an angle of 3.5 to 4 degrees. As it will be seen later these lengths may need to be adjusted during the calculations.

The drawing computer program used must be capable of rotating by a desired angle either the pendulum complex or the escapement wheel around their centres O and O'.

The following working assumptions may be made for the drawing exercise and for the subsequent calculations:

- the pendulum amplitude is nearly equal to the exit angle of the left impulse phase (Figure 4: -0.077 radians); this value or a slightly different value can be tentatively used in the calculation in order to estimate the pendulum angular speed (needed as initial condition for the solution of the pertinent differential equation) at the start of phase 1-2 (position 1); a nominal value of 0,07 r has been used as a tentative value in the following calculations;
- in the free motion phases, the time needed for the contact between an escapement wheel tooth and the locking face of the pallet is determined by the pendulum motion, since the escapement wheel movement can be considered instantaneous.

The calculations for phase 1-2 (left impulse) are here described.

The differential equation used is the following one:

$$\frac{\partial^2 \alpha}{\partial t^2} = \frac{-PW * PL}{PI} * \alpha - \frac{NF}{PI} \times (1.147 - 1.42 * f_d) \quad (1)$$

Which, in the spreadsheet which follow, is written:

$$\left| \frac{\partial^2 \alpha}{\partial t^2} = D * \alpha - H \right. \quad (2)$$

Where:

- α is the angle of the pendulum with reference to the vertical (see Figures 2 to 8)
- PW is the pendulum weight in grams, here assumed to be equal to 45 g
- PL is the pendulum length in cm, here assumed equal to 14.77 cm
- PI is the pendulum inertia moment with reference to the rotation axis (point O in the Figures), estimated equal to 10.02 g s²cm
- NF is the normal force exerted by the escapement wheel tooth on the pallet impulse surface (see Fig.3)
- 1.147 and 1.42 are the lever arms of NF and of the consequent friction force NF*f_d with reference to O
- f_d is the friction factor between wheel and pallet, here assumed equal to 0.08 [British Horological Institute 2007]

NF is given by the formula (Fig. 10):

$$NF = \frac{SM}{5928 * 1.4 * 1.69} \quad (3)$$

Where:

- SM is the spring moment at the barrel periphery, equal in this example to 21000 g cm
- 5928 is the overall reduction ratio of the gear train (see Figure 9)
- 1.4 is a factor depending on the pallet impulse surface angle with the tangent to the escapement wheel external circle drawn from the O centre; in this exercise, this angle has been assumed equal to 45° and the corresponding coefficient 1.4 is

$$1.4 = \frac{1}{\cos(45)} = \frac{1}{0.707} \quad (4)$$

This factor can be different for different clocks (depending on the magnitude of the impulse desired); e.g., for an angle of 55°, this factor would be 1.74 (weaker impulse); the trace of the impulse surface on the drawing plane can also be made non linear, namely curved, and in this case equation (1) would be non-linear and should be solved by numerical methods (a spreadsheet is a simple tool for that)

- 1.69 is the radius of the wheel in cm (Figure 10)

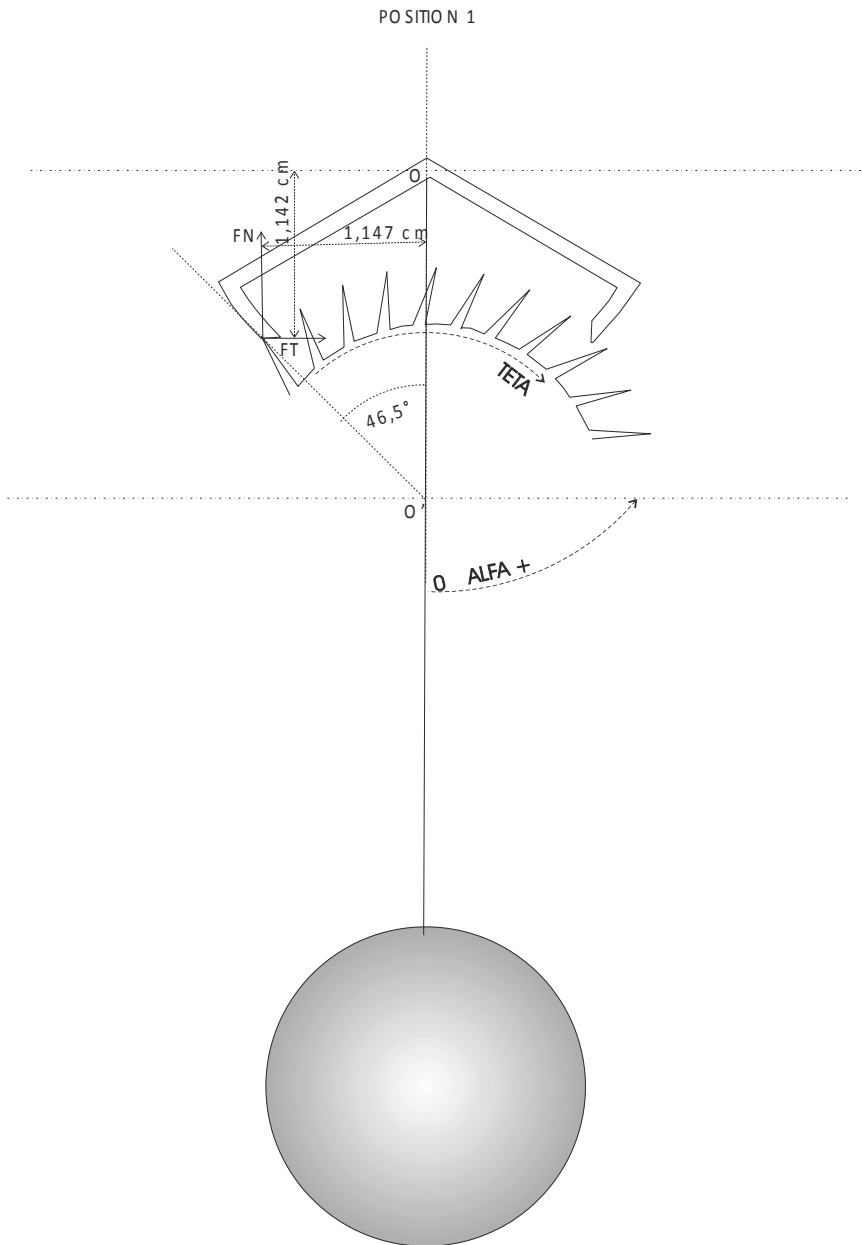


Figure 10 (equal to Fig.3). Normal Force (NF)

At the basis of Equation (1) is the assumption that the inertia of the gear train and the friction in the components of the train itself have no influence on the force transmitted by the wheel teeth to the interacting pendulum pallets: this force, RF (Fig. 10), can be calculated as the static force transmitted by the spring barrel to the escapement wheel in absence of motion. This main assumption of the proposed calculation method gives the possibility to describe the pendulum motion by one equation only. For more precision, two equations should be written: one for the motion of the pendulum and one for the motion of the gear train. Tests in this direction have been made, showing that the second equation is a mere over-complication of the model and that it has no appreciable influence on the results.

Another assumption of Equation (1) is that, for the dimensions of the pendulum chosen (a table pendulum) the hydrodynamic air drag forces have no meaningful influence on the pendulum motion: this assumption has been checked for this case and it may not be true in other cases. The friction of the suspension of the pendulum has been neglected because, as already mentioned, the pendulum is supposed to be supported by a flat spring which can be considered free from energy losses. Further, the pendulum circular error (Rawlings, 1980) has been, for simplicity disregarded here and for the modelling of subsequent phases.

Equation (1), with the above listed numerical data is equivalent to the following one:

$$\left| \frac{\partial^2 \alpha}{\partial t^2} = -66.33 * \alpha - 0.15803 \right. \quad (5)$$

Equation (4) can be solved explicitly [Wylie, 1951] and its solution is:

$$\alpha = C_2 * \sin(8.144 * t) + C_1 * \cos(8.144 * t) - 0.002382 \quad (6)$$

The rotational speed of the pendulum is, then:

$$\frac{\partial \alpha}{\partial t} = C_2 * 8.144 * \cos(8.144 * t) - C_1 * 8.144 * \sin(8.144 * t) \quad (7)$$

The constants C can be calculated from equations (5) and (6) and the initial conditions of the pendulum motion in this phase.

As it is known, the simple pendulum equation of motion for small amplitudes is:

$$\alpha = \alpha_{\max} * \sin\left(\frac{2\pi}{T} * t\right) \quad (8)$$

Where:

- α_{\max} is the amplitude of the pendulum motion, which has tentatively been assumed here equal to 0.07 radians as already mentioned above

- T is the period of the pendulum = $2 * \pi * \sqrt{\frac{PL}{g}}$ (9)

If the length of the pendulum PL (14.77 cm) and the gravity constant of 980 cm/s are introduced, the pendulum period results equal to 0.77 s; consequently, the maximum rotational speed of the pendulum (in POSITION 1, POS. 1) is:

$$\left(\frac{\partial \alpha}{\partial t}\right)_{\max} = \alpha_{\max} * \frac{2\pi}{T} = 0.5712 \text{ r/s} \quad (10)$$

The speed of the pendulum in POS. 1 (equal to its maximum speed) is needed, together with the initial angle of the pendulum, to determine the equation constants C_1 and C_2 .

In POS. 1 (see Fig. 3) α_1 is 0 and $\left(\frac{\partial \alpha}{\partial t}\right)$ is -0.5712 r/s. The time in POS.1 is assumed to be 0 (as at the start of the other Phases of motion in these calculations).

From (5) and (6) the constants result :
 $C_1=0.002382$ and $C_2=-0.07$

The motion of the pendulum can be calculated by the equation solution in an Excel spread sheet. The main results for phase 1 are shown in Figure 11 below.

PW[g]	45	PL[cm]	14,77	PI[gs2cm]	10,02		
fd	0,08						
SM[gcm]	21000	NF[g]	1,497257				
D	-66,3323	PART[r]	0,002378				
		H	0,157741				
t[s]	A[rad]	A'[rad/s]	A''[rad/s ²]	TOTE[gcm]	KINE[gcm]	POTE[gcm]	
0	0	-0,57	0,157741	1,627749	1,627749	0	
0,005	-0,00285	-0,57032	0,346893	1,632264	1,629561	0,002702317	
0,01	-0,0057	-0,56969	0,535994	1,636779	1,625973	0,010806316	
0,015	-0,00855	-0,56812	0,72473	1,641289	1,617008	0,024280713	
0,02	-0,01138	-0,5656	0,912787	1,645783	1,602725	0,043058581	
.....							
0,175	-0,0713	-0,10189	4,886957	1,741251	0,052013	1,689237449	
0,18	-0,07175	-0,07896	4,916955	1,741974	0,031238	1,710735853	
0,185	-0,07209	-0,0559	4,939325	1,742514	0,015658	1,726855922	
0,19	-0,07231	-0,03275	4,95403	1,742868	0,005374	1,737493455	
0,195	-0,07241	-0,00955	4,961045	1,743036	0,000457	1,742579681	
0,2	-0,0724	0,013676	4,960359	1,743019	0,000937	1,742081718	

Figure 11. Excerpts from the spreadsheet for Phase 1-2

In Figure 11 the following new symbols are shown:

- PART (r) is the particular integral of the differential equation (1) in radians

-A indicates α ; A', $\frac{\partial \alpha}{\partial t}$ and A'', $\frac{\partial^2 \alpha}{\partial t^2}$

-KINE, POTE and TOTE are the kinetic energy, the potential energy and the total energy of the pendulum

The main result of the equation solution in the spreadsheet is that for an angle of roughly -0.0724 r the angular speed changes sign and the pendulum tends to stop before the exit angle of the Phase 1 (= -0.077 r, Fig. 4) is reached; this fact means that the impulse received is not sufficient to bring the pendulum to the end position indicated by the tentatively adopted drawing (Fig.4, POS.2): some modification is necessary, either an increase of the force NF exerted by the wheel (increase of the momentum SM or decrease of the multiplication ratio, 5928, of the gear train) or a reduction of the left pallet impulse face length. This last modification is here chosen and the pallet will be modified so that the exit angle of the left impulse phase is -0.724 r in place of -0.77 r; this value will be used in following calculations. This outcome of the Phase 1-2 calculation shows the capability of the proposed model to optimize the clock design, indicating by calculus and not by "trial and error" the nature and measure of the needed modifications.

The main numerical data concerning Phase 1-2 are, then, the following:

$$\alpha_1=0 \text{ r} \quad \alpha_2= -0.0724 \text{ r} \quad \left(\frac{\partial \alpha}{\partial t}\right)_1= -0.57 \text{ r/s} \quad \left(\frac{\partial \alpha}{\partial t}\right)_2 \approx 0 \text{ r/s}$$

$$\theta_1 = 0 \quad \theta_2 = 0.0536 \text{ r} \quad (\text{Fig.3 and 4})$$

$$\text{TOTE}_1 = 1.63 \text{ g cm} \quad \text{TOTE}_2 = 1.74 \text{ g cm}$$

$$t_1 = 0 \text{ s} \quad t_2 = 0.195 \text{ s}$$

The calculation of Phase 2-3 (free, left) follows.

$$\left| \begin{array}{l} \frac{\partial^2 \alpha}{\partial t^2} = \frac{-PW * PL}{PI} * \alpha \end{array} \right. \quad (11)$$

Or, inserting the above listed numerical values:

$$\left| \begin{array}{l} \frac{\partial^2 \alpha}{\partial t^2} = -66.33 * \alpha \end{array} \right. \quad (12)$$

The solution of this equation (free pendulum equation) is:

$$\alpha = C_2 * \sin(8.144 * t) + C_1 * \cos(8.144 * t) \quad (13)$$

And the velocity solution is:

$$\frac{\partial \alpha}{\partial t} = C_2 * 8.144 * \cos(8.144 * t) - C_1 * 8.144 * \sin(8.144 * t) \quad (14)$$

Using $\alpha_2 = -0.0724 \text{ r}$ and $(\frac{\partial \alpha}{\partial t})_2 \approx 0 \text{ r/s}$ (from the solution of Phase 1),

$$C_1 = -0.0724 \text{ and } C_2 = 0$$

$$\alpha(t) = -0.0724 * \cos(8.144t) \quad (15)$$

$$\frac{\partial \alpha}{\partial t} = 0.5839 \sin(8.144 * t) \quad (16)$$

The motion described by (15) and (16) is the free motion of a pendulum with the above listed initial conditions. The final position 3 is identified by the value of α read on the drawings (Fig. 5, $\alpha = -0.679 \text{ r}$).

The main results for Phase 2-3 are shown in Fig. 12 below (the calculation is stopped when the value of $\alpha = -0.679 \text{ r}$ is reached):

t[s]	A[r]	A'[r/s]	TOTE[gcm]	KINE[gcm]	POTE[gcm]
0	-0,072400	0	1,741968	0	1,741968
0,0005	-0,072399	0,002401	1,741968	2,89E-05	1,741939
0,001	-0,072398	0,004802	1,741968	0,000116	1,741852
0,0015	-0,072395	0,007203	1,741968	0,00026	1,741708
0,002	-0,072390	0,009603	1,741968	0,000462	1,741506
0,0025	-0,072385	0,012004	1,741968	0,000722	1,741246
.....					
0,0415	-0,068304	0,195507	1,741946	0,191497	1,550449
0,042	-0,068206	0,197771	1,741945	0,195957	1,545988
0,0425	-0,068106	0,200031	1,741945	0,200462	1,541483
0,043	-0,068006	0,202288	1,741944	0,205011	1,536934
0,0435	-0,067904	0,204541	1,741944	0,209604	1,53234
0,044	-0,067801	0,206791	1,741943	0,214241	1,527702

Figure 12. Excerpts from the spreadsheet for Phase 2-3

The main numerical data concerning Phase 2-3 are the following:

$$\alpha_2 = -0.0724 \text{ r} \quad \alpha_3 = -0.0679 \text{ r} \quad \left(\frac{\partial \alpha}{\partial t}\right)_1 = 0 \text{ r/s} \quad \left(\frac{\partial \alpha}{\partial t}\right)_2 \approx 0.205 \text{ r/s}$$

$$\theta_2 = 0.0536 \text{ r} \quad \theta_3 = 0.0886 \text{ r} \text{ (Fig. 4 and 5)}$$

$$\text{TOTE}_2 = 1.74 \text{ g cm} \quad \text{TOTE}_3 = 1.74 \text{ g cm}$$

$$t_2 = 0.195 \text{ s} \quad t_3 = 0.2335 \text{ s}$$

The calculation of Phase 3-4 (lock, right) follows.

$$\left| \frac{\partial^2 \alpha}{\partial t^2} = \frac{-PW * PL}{PI} * \alpha - \frac{NF}{PI} \times (1.6 * f_d) \right. \quad (17)$$

Where the coefficient 1.6 is the lever arm of the friction force with respect to fulcrum O. The solution of (17) is

$$\alpha = C_2 * \sin(8.144 * t) + C_1 * \cos(8.144 * t) - 0.000286 \quad (18)$$

And, consequently,

$$\frac{\partial \alpha}{\partial t} = C_2 * 8.144 * \cos(8.144 * t) - C_1 * 8.144 * \sin(8.144 * t) \quad (19)$$

As usual, using the values of α and of its first derivative for position 3 from the previous calculation, the two constants can be calculated:

$$C_1 = -0.0676 \quad C_2 = 0.025$$

The solution for α and for the rotational speed is, then:

$$\alpha = 0.025 * \sin(8.144 * t) - 0.0676 * \cos(8.144 * t) - 0.000286 \quad (20)$$

$$\frac{\partial \alpha}{\partial t} = 0.025 * 8.144 * \cos(8.144 * t) + 0.0676 * 8.144 * \sin(8.144 * t) \quad (21)$$

The relevant parts of the pertinent spreadsheet are (Fig. 13):

t[s]	A[r]	A'[r/s]	TOTE[gcm]	KINE[gcm]	POTE[gcm]
0	-0,06789	0,2036	1,739202	0,207679	1,531523
0,0005	-0,06778	0,20584	1,739182	0,212274	1,526908
0,001	-0,06768	0,208077	1,739162	0,216913	1,522249
0,0015	-0,06758	0,21031	1,739141	0,221594	1,517548
0,002	-0,06747	0,21254	1,739121	0,226317	1,512803
0,0025	-0,06736	0,214766	1,7391	0,231083	1,508017
0,003	-0,06726	0,216989	1,739079	0,235891	1,503188
.....					
0,03	-0,05983	0,330726	1,737632	0,547992	1,18964
0,0305	-0,05967	0,332698	1,7376	0,554546	1,183054
0,031	-0,0595	0,334664	1,737567	0,561121	1,176447
0,0315	-0,05933	0,336625	1,737535	0,567715	1,169819
0,032	-0,05916	0,33858	1,737502	0,574329	1,163172
0,0325	-0,05899	0,34053	1,737469	0,580963	1,156506

Figure 14. Excerpts from the spreadsheet for Phase 3-4

From the drawings (Fig. 6 for POS.4), the final value of α is -0.059 and, from the spreadsheet, the corresponding relative time (time 0 is assumed to be at the start of each Phase) is 0.032 s (total time = 0.2335+0.32=0.2655 s). The corresponding speed is 0.3386 r/s).

The main numerical data concerning Phase 3-4 are the following:

$$\alpha_3 = -0.0679 \text{ r} \quad \alpha_4 = -0.059 \text{ r} \quad \left(\frac{\partial \alpha}{\partial t}\right)_3 = 0.2335 \text{ r/s} \quad \left(\frac{\partial \alpha}{\partial t}\right)_4 \approx 0.3386 \text{ r/s}$$

$$\theta = 0.0886 \text{ r} \quad \theta_4 = 0.0886 \text{ r} \quad (\text{Fig. 5 and 6})$$

$$\text{TOTE}_3 = 1.74 \text{ g cm} \quad \text{TOTE}_4 = 1.74 \text{ g cm}$$

$$t_3 = 0.2335 \text{ s} \quad t_4 = 0.2655 \text{ s}$$

The calculation of Phase 4-5 (impulse, right) follows.

The main equation is similar to that for Phase 1-2, with the necessary changes in signs and coefficients (Fig. 6 and 7)

$$\frac{\partial^2 \alpha}{\partial t^2} = \frac{-PW * PL}{PI} * \alpha + \frac{NF}{PI} \times (1.176 - 1.12 * f_d) \quad (22)$$

Which leads to:

$$\frac{\partial^2 \alpha}{\partial t^2} = -66.33 * \alpha + 0.1626 \quad (23)$$

The solution of the equation is:

$$\alpha = C_2 * \sin(8.144 * t) + C_1 * \cos(8.144 * t) + 0.00245 \quad (24)$$

The rotational speed of the pendulum is, then:

$$\frac{\partial \alpha}{\partial t} = C_2 * 8.144 * \cos(8.144 * t) - C_1 * 8.144 * \sin(8.144 * t) \quad (25)$$

The constants C can be calculated from equations (24) and (25) and the initial conditions of the pendulum motion in this phase.

In POS. 4 (see Fig. 6 and Fig. 14) α_4 is -0.059 and $(\frac{\partial \alpha}{\partial t})$ is 0.34 r/s. The time in POS.4 is

assumed to be 0 (as at the start of the other Phases of motion).

From (24) and (25) the constants result :

$C_1 = -0.063$ and $C_2 = -0.039$

The maximum angle at the exit of the Phase 4-5 is equal to 0.43 r (Fig.7) and the relevant portions of the spreadsheet are shown in Fig. 15

PW[g]	45	PL[cm]	14,77	PI[gs2cm]	10,02		
fs	0,08						
MS[gcm]	21000	NF[g]	1,497257				
D	66,33233533	PART[r]	0,002447				
		H	0,162337				
t[s]	A[rad]	A'[rad/s]	A''[rad/s ²]	TOTE[gcm]	KINE[gcm]	POTE[gcm]	
0	-0,05905	0,342048	4,079262	1,744939	0,586154	1,158784873	
0,003	-0,058005604	0,354182	4,009984	1,746635	0,628478	1,118157329	
0,006	-0,056925122	0,366104	3,938314	1,748389	0,6715	1,076889021	
0,009	-0,055809199	0,377807	3,864292	1,750202	0,71512	1,035081618	
0,012	-0,054658502	0,389286	3,787963	1,75207	0,759232	0,992838175	
0,015	-0,053473718	0,400531	3,709374	1,753994	0,803732	0,950262891	
.....							
0,171	0,032885394	0,553549	-2,01903	1,894537	1,535145	0,359392591	
0,174	0,034536792	0,547328	-2,12857	1,89723	1,500836	0,396393928	

0,177	0,036169037	0,540781	-2,23684	1,899892	1,465145	0,434747301
0,18	0,037781155	0,533911	-2,34377	1,902522	1,428156	0,474365911
0,183	0,039372184	0,526722	-2,44931	1,905117	1,389957	0,515159878
0,186	0,040941175	0,519219	-2,55339	1,907676	1,35064	0,557036458
0,189	0,042487191	0,511406	-2,65594	1,910198	1,310298	0,599900256
0,192	0,044009309	0,503288	-2,7569	1,912682	1,269028	0,643653455

Figure 15. Excerpts from the spreadsheet for Phase 4-5

The main numerical data concerning Phase 4-5 are the following:

$$\alpha_4 = -0.059 \text{ r} \quad \alpha_5 = 0.043 \text{ r} \quad \left(\frac{\partial \alpha}{\partial t}\right)_4 = 0.34 \text{ r/s} \quad \left(\frac{\partial \alpha}{\partial t}\right)_5 = 0.51 \text{ r/s}$$

$$\theta_4 = 0.0886 \text{ r} \quad \theta_5 = 0.1586 \quad (\text{Fig. 6 and 7})$$

$$\text{TOTE}_4 = 1.74 \text{ g cm} \quad \text{TOTE}_5 = 1.9 \text{ g cm}$$

$$t_4 = 0.2655 \text{ s} \quad t_5 = 0.4545 \text{ s}$$

The calculation of Phase 5-6 (free, right, Fig. 7 and 8) follows.

The main equation is equal to that for Phase 2-3.

$$\frac{\partial^2 \alpha}{\partial t^2} = \frac{-PW * PL}{PI} * \alpha \quad (26)$$

Or, inserting the above listed numerical values:

$$\frac{\partial^2 \alpha}{\partial t^2} = -66.33 * \alpha \quad (27)$$

The solution of this equation (free pendulum equation) is:

$$\alpha = C_2 * \sin(8.144 * t) + C_1 * \cos(8.144 * t) \quad (28)$$

And the velocity solution is:

$$\frac{\partial \alpha}{\partial t} = C_2 * 8.144 * \cos(8.144 * t) - C_1 * 8.144 * \sin(8.144 * t) \quad (29)$$

Using $\alpha_5 = 0.043 \text{ r}$ and $\left(\frac{\partial \alpha}{\partial t}\right)_5 = 0.51 \text{ r/s}$ (from the solution of Phase 4-5),

$$C_1 = 0.043 \text{ and } C_2 = 0.063$$

$$\alpha(t) = 0.063 * \sin(8.144 * t) + 0.043 * \cos(8.144 * t) \quad (30)$$

$$\frac{\partial \alpha}{\partial t} = 0.063 * 8.144 * \cos(8.144 * t) - 0.043 * 8.144 * \sin(8.144 * t) \quad (31)$$

The motion described by (30) and (31) is the free motion of a pendulum with the above listed initial conditions. The final position α_6 is identified by the value of α read on the drawings (Fig. 8, $\alpha = 0.0596$ r).

The main results for Phase 5-6 are shown in Fig. 16 below:

	A[r]	A'[r/s]	A''[r/s ²]	TOTE[gcm]	KINE[gcm]	POTE[gcm]
0	0,043000	0,513072	-2,85229	1,933316	1,318847	0,614469
0,005	0,045529	0,498391	-3,02005	1,933324	1,244451	0,688873
0,01	0,047983	0,482883	-3,18279	1,933332	1,168213	0,76512
0,015	0,050357	0,466575	-3,34026	1,933341	1,090638	0,842702
0,02	0,052647	0,449493	-3,4922	1,933349	1,012241	0,921107
0,025	0,054850	0,431666	-3,63834	1,933357	0,933542	0,999815
0,03	0,056962	0,413123	-3,77845	1,933364	0,855062	1,078303
0,035	0,058980	0,393896	-3,9123	1,933372	0,777321	1,156051
0,04	0,060900	0,374015	-4,03966	1,933379	0,700834	1,232545

Figure 16. Excerpts from the spreadsheet for Phase 5-6

The main numerical data concerning Phase 5-6 are the following:

$$\alpha_5 = 0.063 \text{ r} \quad \alpha_6 = 0.0596 \text{ r} \quad \left(\frac{\partial \alpha}{\partial t}\right)_5 = 0.51 \text{ r/s} \quad \left(\frac{\partial \alpha}{\partial t}\right)_6 = 0.39 \text{ r/s}$$

$$\theta_5 = 0.1586 \text{ r} \quad \theta_6 = 0.1936 \quad (\text{Fig. 7 and 8})$$

$$\text{TOTE}_5 = 1.9 \text{ g cm} \quad \text{TOTE}_6 = 1.93 \text{ g cm}$$

$$t_5 = 0.4545 \text{ s} \quad t_6 = 0.495 \text{ s}$$

The calculation of Phase 6-1 (lock, left) follows.

The main equation is similar to that for Phase 3-4, with the necessary changes in signs and coefficients (Fig. 8 and 3).

In particular, in this Phase and for this sample clock, the pendulum swings to the right for the first part of the Phase and to the left for the second part. For this reason the equation of motion is different for the two sub-phases (named here Phase 6-1' and Phase 1'-1). If the solution of the equations is obtained by a numerical method,

the two equations can be unified by the addition of a coefficient $\frac{|\alpha|}{\alpha}$ in place of the sign which is different by the two equations (see later). If an analytical solution is preferred (as in this case), the equations are two and two sub-phases have to be studied.

The equations and solutions for sub-Phase 6-1' follow.

$$\left| \frac{\partial^2 \alpha}{\partial t^2} = \frac{-PW * PL}{PI} * \alpha - \frac{NF}{PI} \times (1.6 * f_d) \right. \quad (32)$$

Where the coefficient 1.6 is the lever arm of the friction force with respect to fulcrum O.

The solution of (32) is

$$\alpha = C_2 * \sin(8.144 * t) + C_1 * \cos(8.144 * t) - 0.000289 \quad (33)$$

And, consequently,

$$\frac{\partial \alpha}{\partial t} = C_2 * 8.144 * \cos(8.144 * t) - C_1 * 8.144 * \sin(8.144 * t) \quad (34)$$

As usual, using the values of α and of its first derivative for position 6, the two constants can be calculated:

$$C_1 = 0.0599 \quad C_2 = 0.048$$

The solution for α and for the rotational speed is, then:

$$\alpha = 0.0394 * \sin(8.144 * t) + 0.0599 * \cos(8.144 * t) - 0.000289 \quad (35)$$

$$\frac{\partial \alpha}{\partial t} = 0.0394 * 8.144 * \cos(8.144 * t) - 0.0599 * 8.144 * \sin(8.144 * t) \quad (36)$$

The relevant parts of the pertinent spreadsheet are (Fig. 17):

t[s]	A[r]	A'[r/s]	ETOT[gcm]	ECIN[gcm]	EPOT[gcm]
0	0,059611	0,320874	1,696736	0,515829	1,180907
0,005	0,061183	0,300782	1,697268	0,453254	1,244014
0,01	0,062636	0,280192	1,697109	0,393322	1,303787
0,015	0,063984	0,259137	1,696962	0,336431	1,360531
0,02	0,065226	0,237653	1,696827	0,282958	1,413869
0,025	0,06636	0,215774	1,696704	0,233258	1,463446
.....					
0,04	0,069093	0,14814	1,696407	0,109947	1,586459
0,045	0,069776	0,125054	1,696332	0,078349	1,617983
0,05	0,070343	0,101761	1,696271	0,05188	1,644391
0,055	0,070793	0,078299	1,696222	0,030715	1,665507
0,06	0,071126	0,054707	1,696186	0,014994	1,681192
0,065	0,07134	0,031024	1,696163	0,004822	1,691341
0,07	0,071436	0,00729	1,696152	0,000266	1,695886
0,075	0,071413	-0,01646	1,696155	0,001357	1,694798

Figure 17. Excerpts from the spreadsheet for Phase 6-1'

From Fig.17 above, the velocity changes sign at relative time 0.07s and the corresponding value of α is 0.071 r (end of Phase 6-1'). The rotational velocity is 0 as above explained.

The main numerical data concerning Phase 6-1' are the following:

$$\alpha_6 = 0.0596 \text{ r} \quad \alpha_{1'} = 0.071 \text{ r} \quad \left(\frac{\partial \alpha}{\partial t}\right)_6 = 0.394 \text{ r/s} \quad \left(\frac{\partial \alpha}{\partial t}\right)_{1'} \approx 0 \text{ r/s}$$

$$\theta_6 = 0.1936 \text{ r} \quad \theta_{1'} = 0.1936 \text{ r} \quad (\text{Fig. 8 and 3})$$

$$\text{TOTE}_6 = 1.93 \text{ g cm} \quad \text{TOTE}_{1'} = 1.69 \text{ g cm}$$

$$t_6 = 0.495 \text{ s} \quad t_{1'} = 0.565 \text{ s}$$

The equations and solution for sub-Phase 1'-1 follow.

$$\left| \frac{\partial^2 \alpha}{\partial t^2} = \frac{-PW * PL}{PI} * \alpha + \frac{NF}{PI} \times (1.6 * f_d) \right. \quad (37)$$

Where the coefficient 1.6 is the lever arm of the friction force with respect to fulcrum O.
The solution of (37) is

$$\alpha = C_2 * \sin(8.144 * t) + C_1 * \cos(8.144 * t) - 0.00017 \quad (38)$$

And, consequently,

$$\frac{\partial \alpha}{\partial t} = C_2 * 8.144 * \cos(8.144 * t) - C_1 * 8.144 * \sin(8.144 * t) \quad (39)$$

As usual, using the values of α and of its first derivative for position 1', the two constants can be calculated:

$$C_1 = 0.071 \quad C_2 = 0$$

The solution for α and for the rotational speed is, then:

$$\alpha = 0.071 * \cos(8.144 * t) + 0.00017 \quad (40)$$

$$\frac{\partial \alpha}{\partial t} = -0.071 * 8.144 * \sin(8.144 * t) \quad (41)$$

The relevant parts of the pertinent spreadsheet are (Fig. 18):

t[s]	A[r]	A'[r/s]	TOTE[gcm]	KINE[gcm]	POTE[gcm]
0	0,07117	0	1,683282	0	1,683282
0,005	0,071111	-0,02354	1,683275	0,002776	1,680499
0,01	0,070935	-0,04704	1,683254	0,011085	1,672169
0,015	0,070641	-0,07046	1,68322	0,024873	1,658347
0,02	0,07023	-0,09377	1,683171	0,044048	1,639124
.....					
0,175	0,010471	-0,57211	1,676236	1,6398	0,036436
0,18	0,007603	-0,57505	1,67591	1,656702	0,019208
0,185	0,004722	-0,57703	1,675583	1,668173	0,00741
0,19	0,001834	-0,57807	1,675256	1,674139	0,001118
0,195	-0,00106	-0,57814	1,674929	1,674558	0,000371
0,2	-0,00395	-0,57725	1,674604	1,669429	0,005174

Figure 18. Excerpts from the spreadsheet for Phase 1'-1

From the drawings (Fig. 3 for POS.1), the final value of α is 0 and, from the spreadsheet, the corresponding relative time (time 0 is assumed to be at the start of each Phase) is 0.19 s (total time = 0.565+0.19=0.755 s). The corresponding speed is -0.58 r/s).

The main numerical data concerning Phase 1'-1 are the following:

$$\alpha_{1'}=0.071 \text{ r} \quad \alpha_1= 0 \text{ r} \quad \left(\frac{\partial\alpha}{\partial t}\right)_{1'}=0 \text{ r/s} \quad \left(\frac{\partial\alpha}{\partial t}\right)_1=-0.578 \text{ r/s}$$

$$\theta_{1'}= 0.1936 \text{ r} \quad \theta_1= 0.1936 \text{ r} \quad (\text{Fig. - })$$

$$\text{TOTE}_{1'} = 1.68 \text{ g cm} \quad \text{TOTE}_1= 1.67 \text{ g cm}$$

$$t_{1'} = 0.565\text{s} \quad t_1 = 0.76 \text{ s}$$

The main discrepancies of these calculations from the initially assumed values are:

- the duration of one complete cycle of the pendulum is 0.76 s instead of the initially assumed 0.77 s (pendulum period on the basis of pendulum length)
- the angular speed in Position 1 results 0.578 r/s instead of 0.512 r/s initially assumed
- the final total energy of the pendulum is 1.67 g cm instead of the initially assumed 1.63 g cm.

Given the character of example of the calculations performed, the results are acceptable. If more precision is desired, the calculations may be repeated with augmented precision (decimal figures considered) and a second iteration can be made: this exercise would show that the calculations tend to converge towards a stable situation. The property of isochronism of the pendulum for small oscillation amplitudes plays its role in this connection. The same is true for any oscillating mechanism controlled by a linear regulator; therefore, also a watch controlled by a linear balance oscillator would behave in the same way.

Figures 19, 20, 21, 22 show a summary of the most relevant results of the above discussed calculations.

TIME	ALFA	TIME	ENERGY	TIME	TETA[r]	TIME	SINALFA	POSITION
0	0	0	1,63	0	0	0	0	ONE
0,195	-0,0724	0,195	1,74	0,195	0,0536	0,195	-0,07234	TWO
0,2335	-0,0679	0,2335	1,74	0,2335	0,0886	0,2335	-0,06777	THREE
0,2655	-0,059	0,2655	1,74	0,2655	0,0886	0,2655	-0,05875	FOUR
0,4545	0,043	0,4545	1,9	0,4545	0,1586	0,4545	0,041819	FIVE
0,495	0,0596	0,495	1,93	0,495	0,1936	0,495	0,058918	SIX
0,565	0,08	0,565	1,68	0,565	0,1936	0,565	0,072338	ONE'
0,76	0	0,76	1,67	0,76	0,1936	0,76	1,34E-05	ONE

Figure 19. Summary of the main results of the calculations performed

For comparison, the column SINALFA has been added to the calculation results: it represents a simple SINE function with the same period of the pendulum.

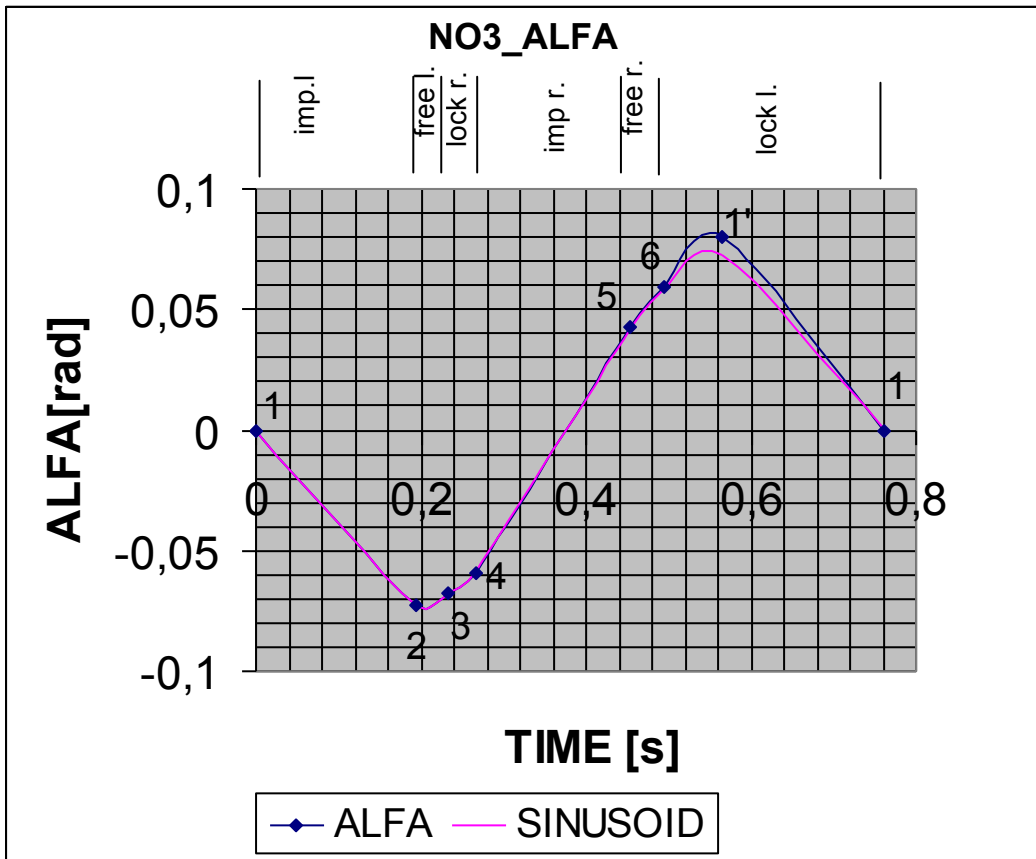


Figure 20. Calculated α (ALFA), pendulum angle with the vertical as a function of time

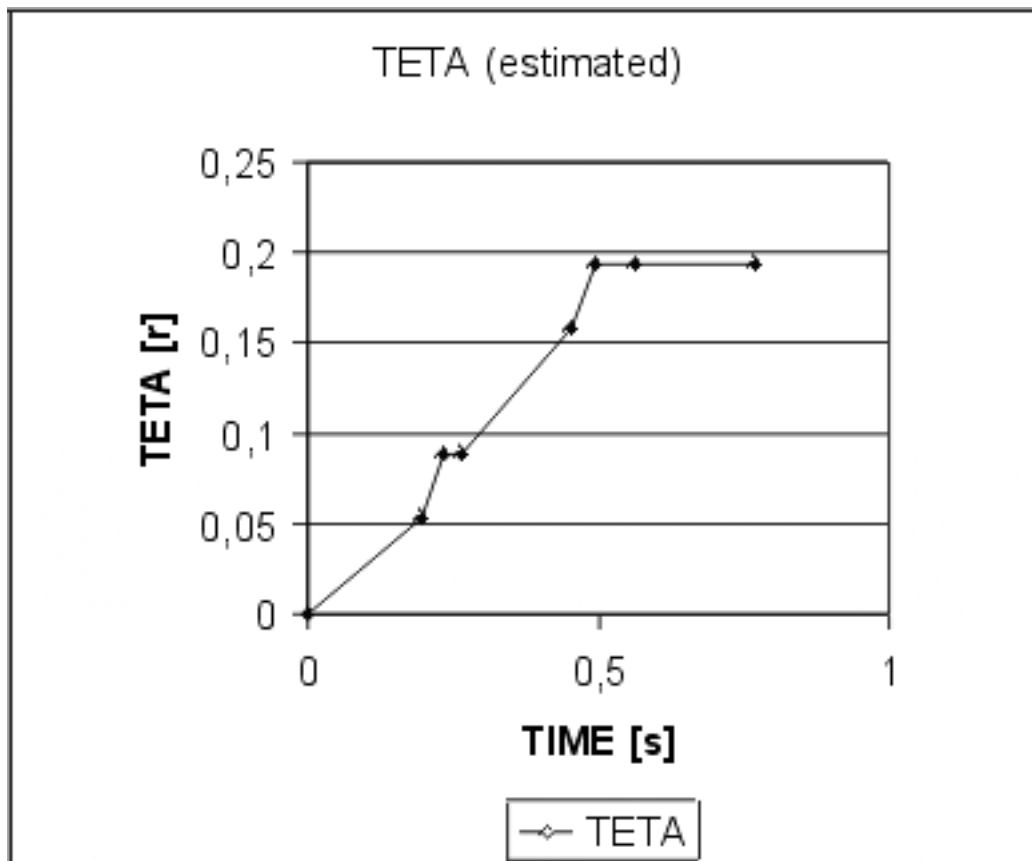


Figure 21. Escapement wheel angle θ (TETA) with reference to Position 1 as a function of time

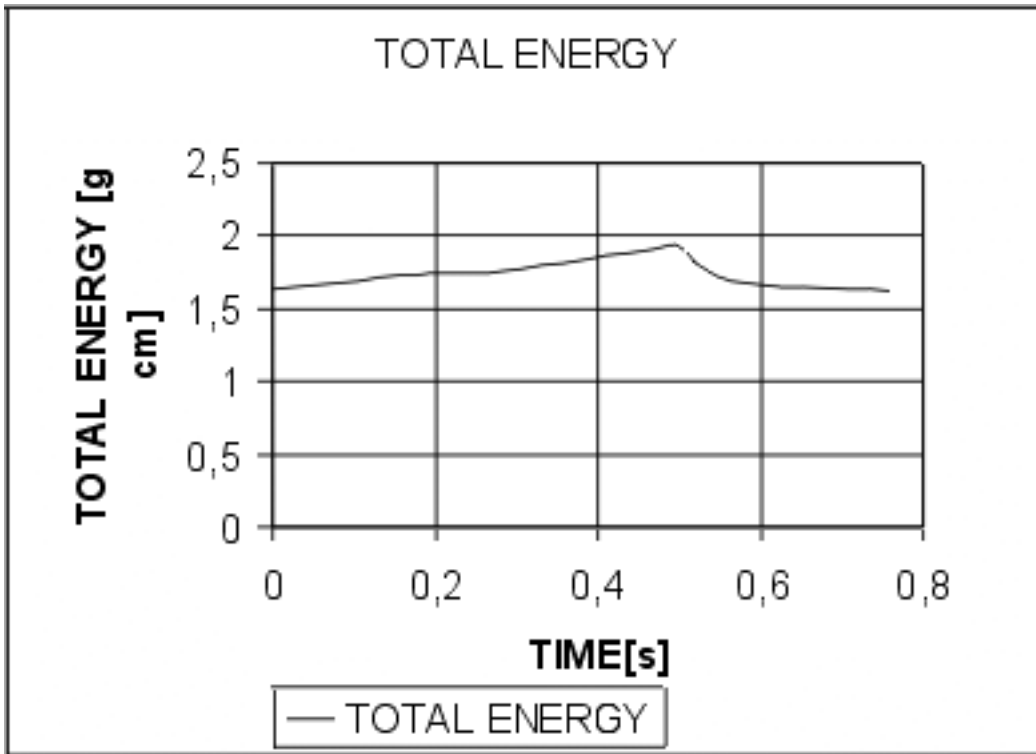


Figure 22. Total energy of the pendulum as a function of time

The question of how accurate is the example clock studied above is easily answered.

Since the total escapement wheel angle θ (TETA) in one period is (Fig. 19) 0.1936 r , the average angular speed of the wheel is $0.1936/0.76 = 0.255 \text{ r/s}$ (the period resulting from Fig. 19 is 0.76 s).

The reduction ratio between the central (minutes) wheel and the escapement wheel is (Fig. 9) $10 \cdot 12 = 120$; therefore the angular speed of the central wheel is $0.255/120 = 0.002 \text{ r/s} = 0.115^\circ/\text{s}$.

In one hour the rotated angle is, therefore, $0.115 \cdot 3600 = 412^\circ$ and not 360° as it should be in an accurate clock. This inaccuracy is clearly unacceptable (ratio of $412/360 = 114\%$) and, therefore, some correction to the clock design and some adjustment to it must be introduced. Two main actions can be taken:

- a change in the reduction ratio between the escapement and the central wheels
- a change in the pendulum length

Since the adjustment of the pendulum length is an accurate but limited operation (the adjustment length on the dimension chosen is of the order of 1 cm , while a variation of the order of 3.5 cm would be required in this case) both the above listed actions must be taken. As an example, the increase of the reduction ratio from 120 to 140 would imply a speed of the minute wheel of $370.8^\circ/\text{h}$. The remaining inaccuracy of about 3% could be accommodated by an increase of the pendulum length of 0.86 cm (length of 15.63 cm instead of 14.77 cm).

As a matter of completeness, the Q ("Quality") value (Rawlings, 1993) which can be calculated by the data of Figure 19 is

$$Q = \pi * \frac{E}{\Delta E} = \pi * 1.67 / (1.67 - 1.63) = 131 \quad (42)$$

This value would probably result higher for subsequent and more precise iterations beyond the first one presented in this paper.

6. POSSIBLE USES OF THE MODEL AND IMPROVEMENTS

As above said a model like the one presented can be useful for teaching and for clock design and repair. The model can be improved in the following directions:

- using two equation instead of one (one in the unknown α and one in the unknown θ); the link between the two equations in the impulse phases can be a geometrical one (introducing a fixed ratio between α and θ during the contact between the escapement wheel and the pallet face in the impulse phases); this modification can take into account the inertia of the gear train but it has no significant advantage on the single-equation method used here which implies neglecting the gear train friction, the air drag and inertia);
- taking into account the pendulum circular error (Rawlings, 1980), by the use of the function $\sin \alpha$ instead of α in the second member of equation (1) and of following similar equations for the other Phases of motion of the pendulum
- making the calculation of the various Phases more automatic with the creation, for example, of an Excel macro in order to make calculations and, in particular, iterations less time consuming.

7. CONCLUSIONS

Simple mathematical models of the escapement mechanism of a clock or watch can be developed. One of these models is presented and used in this paper. An example table clock is chosen as a test case: it doesn't correspond to a real clock since the various dimensions and properties have been extracted from different sources. The calculation performed demonstrates the capability of the proposed model to give a good insight in the properties and behaviour of a clock or watch. Improvements are obviously possible in various directions.

REFERENCES

- Beléndez A. et al., Exact solution for the nonlinear pendulum, *Revista Brasileira de Ensino de Física*, v.29, n. 4, p.645, 2007
- British Horological Institute, *The practical Lubrication of Clocks and Watches*, BHI Ltd, Upton Hall, NG23 5TE, 2007
- De Carle D., *Watch and Clock Encyclopedia*, Biddles Limited, King's Lynn, Norfolk, 2008
- De Carle D., *L'Orologiaio Riparatore*, Hoepli, Milano, 2002
- Gelsey A., *Automated Physical Modeling*, Yale University New Haven Conn., 06520-2158
- Headrick M.V., *Clock and Watch Escapements Mechanics*, <http://www.geocities.com/mvhw/>, 2012

Le Lionnais Francois, Le Temps, Robert Delpire, Paris 1959

Lepschy A.M. et al., Feedback Control in Ancient Water and Mechanical Clocks, IEEE Transactions on Education, Vol. 35, No. 1, Feb. 1992

Moon F.C. and Stiefel P.D., Philosophical Transactions of The Royal Society, vol 364 no. 1846, 2006, Coexisting chaotic and periodic dynamics in clock escapements.

Popkonstantinovic B. et al., 3D Modeling and Motion Analysis of the Clock Mechanism, 13th World Congress in Mechanism and Machine Science, Guanajuato, Mexico, 2001

Rawlings A.L., The Science of Clocks and Watches, Pitman Publishing Corporation 1980, 1993

Schwartz C. and Gran R., Describing Function Analysis Using Matlab and Simulink, IEEE Control System Magazine, 2001

www.britannica.com, Pendulum, 2012

Wylie, C.R. Jr., Advanced Engineering Mathematics, Mc Graw Hill Book Co., New York, 1951